Construction and Building Materials 65 (2014) 140–150

Contents lists available at ScienceDirect

Construction and Building Materials

journal homepage: www.elsevier.com/locate/conbuildmat

Effect of nano-silica on the hydration and microstructure development of Ultra-High Performance Concrete (UHPC) with a low binder amount

R. Yu *, P. Spiesz, H.J.H. Brouwers

Department of the Built Environment, Eindhoven University of Technology, P.O. Box 513, 5600 MB Eindhoven, The Netherlands

HIGHLIGHTS

- A dense skeleton of UHPC can be obtained with a relatively low binder amount.
- To get the highest mechanical properties, an optimal amount of nano-silica is calculated.
- The combined effect of SP and nano-silica additions on the hydration of UHPC is analyzed.
- The mechanism of the microstructure development of UHPC is analyzed.

ARTICLE INFO

Article history:
Received 17 January 2014
Received in revised form 21 March 2014
Accepted 4 April 2014

Keywords:
Ultra-High Performance Concrete (UHPC)
Low binder amount
Nano-silica
Hydration
Microstructure development

ABSTRACT

This paper presents the effect of nano-silica on the hydration and microstructure development of Ultra-High Performance Concrete (UHPC) with a low binder amount. The design of UHPC is based on the modified Andreasen and Andersen particle packing model. The results reveal that by utilizing this packing model, a dense and homogeneous skeleton of UHPC can be obtained with a relatively low binder amount (about 440 kg/m^3). Moreover, due to the high amount of superplasticizer utilized to produce UHPC in this study, the dormant period of the cement hydration is extended. However, due to the nucleation effect of nano-silica, the retardation effect from superplasticizer can be significantly compensated. Additionally, with the addition of nano-silica, the viscosity of UHPC significantly increases, which causes that more air is entrapped in the fresh mixtures and the porosity of the hardened concrete correspondingly increases. In contrary, due to the nucleation effect of nano-silica, the hydration of cement can be promoted and more C–S–H gel can be generated. Hence, it can be concluded that there is an optimal nano-silica amount for the production of UHPC with the lowest porosity, at which the positive effect of the nucleation and the negative influence of the entrapped air can be well balanced.

1. Introduction

In recent years, with the development of new plasticizing concrete admixtures and fine pozzolanic materials, it has become possible to produce high performance concrete (HPC) or even Ultra-High Performance Concrete (UHPC). For the production of UHPC, the pozzolanic materials (silica fume, ground granulated blast-furnace slag, fly ash) are widely utilized [1–3]. Due to its high purity and high specific surface area, the pozzolanic reaction of silica fume is fast and could more effectively promote the strength development of concrete, compared to the other pozzolanic materials [4]. Nevertheless, the new developments of nano-technology guarantee that various forms of nano-sized amorphous silica can be produced, which have higher specific surface areas and activities compared to conventional silica fume [5,6]. Hence, a considerable investigation effort has been paid on clarifying their effect on the properties of concrete.

In the available literature it can be found that with the addition of nano-silica in cement or concrete, even at small dosages, nano-silica can significantly improve the mechanical properties of cementitious materials [7]. For instance, Nazari and Riahi [8] showed that a 70% compressive strength improvement of concrete can be achieved with an addition of 4% (by mass of cement) of nano-silica. Li et al. [9] found that when 3% and 5% nano-silica were added to plain cement mortar, the compressive strength increased by 13.8% and 17.5% at 28 days, respectively. However, some contradictory experimental results can also be found in the literature. For example, Senff et al. [10] found that the contribution of nano-SiO_2, nano-TiO_2, and nano-SiO_2 plus nano-TiO_2 defined by factorial design, did not lead to any significant effect on the compressive strength. Moreover, they also found that the values

* Corresponding author. Tel.: +31 (0) 40 247 5469; fax: +31 (0) 40 243 8595.
E-mail address: r.yu@tue.nl (R. Yu).

http://dx.doi.org/10.1016/j.conbuildmat.2014.04.063
0950-0618/

Nomenclature

D_{max}	maximum particle size (μm)
D_{min}	minimum particle size (μm)
f_c	compressive strength of UHPC at 28 days (N/mm^2)
K_t	strength improvement (%)
m_{binder}	total mass of the used binder (kg)
m_d	mass of oven dried sample (g)
m_s	mass of surface dried and water-saturated sample in air (g)
m_w	hydrostatic mass of water-saturated sample (g)
M_{CaCO_3}	mass change of UHPC paste caused by the decomposition of $CaCO_3$ (g)
M_i	mass of the fraction i in solid materials (g)
M_j	mass of the fraction j in liquid materials (g)
M'_{Water}	mass of non-evaporable water (g)
$M_{Water\text{-}Full}$	water requirement for full hydration cement (g)
M_{105}	mass of UHPC paste after heat treatment at 105 °C for 2 h (g)
M_{1000}	mass of UHPC paste after heat treatment at 1000 °C for 2 h (g)
P_{mix}	composed mix curve
P_{tar}	target curve
q	distribution modulus
RSS	sum of the squares of the residuals
S_i	strength of UHPC with nano-silica (i corresponds to nano-silica amount) (MPa)
S_0	strength of UHPC without nano-silica (reference sample) (MPa)
$V_{container}$	volume of the container (cm^3)
V_{liquid}	volume of liquid in the container (cm^3)
V_{solid}	volume of solid particles in the container (cm^3)
X_{binder}	binder efficiency (N/mm^2)/(kg/m^3)
β_t	degree of cement hydration at hydration time t (days) (%)
$\varphi_{v,water}$	water-permeable porosity (%)
ϕ_{air}	air content in UHPC (%)
ρ_i	density of the fraction i in solid materials (g/cm^3)
ρ_j	density of the fraction j in liquid materials (g/cm^3)

of torque, yield stress and plastic viscosity of mortars with nano-additives increased significantly. According to the experimental results of Ltifi [11], even a lower compressive strength of samples with 3% nano-silica can be observed, compared to the plain specimens. The difference of these experimental results should be attributed to the basic characteristics of the nano-silica (e.g. pozzolanic activity, specific surface area). To interpret the influence of nano-silica on the cement hydration, some theoretical mechanisms can be found in the available literature. For example, Land and Stephan [5] observed that the hydration heat of Ordinary Portland Cement blended with nano-silica in the main period increases significantly with an increasing surface area of silica. Thomas et al. [12] showed that the hydration of tri-calcium silicate (C_3S) can be accelerated by the addition of nano-scaled silica or C–S–H-particles. Björnström et al. [6] monitored the hydration process of C_3S pastes and the accelerating effects of a 5 nm colloidal silica additive on the rate of C_3S phase dissolution, C–S–H gel formation and removal of non-hydrogen bound OH groups. However, it can be noticed that the investigation of the effect of nano-silica on cement hydration and microstructure development of UHPC is insufficient [13]. This should be owed to the fact that the nano-silica is still a relatively new material for the application in high performance concrete, and its price is much higher compared to that of silica fume or other pozzolanic materials [14]. Additionally, for the production of UHPC, the water/binder ratio is relatively low and a large amount of superplasticizer is commonly used, which means it is not suitable to predict the pozzolanic activity of nano-silica at low water/binder ratio, based on the experimental results that are obtained for high water/binder ratios. Therefore, how the additional nano-silica influences the cement hydration and microstructure development of UHPC remains an open question.

As commonly known, the cement production is said to represent about 7% of the total anthropogenic CO_2 emissions [15–17]. Hence, one of the key sustainability challenges for the next decades is to design and produce concrete with less clinker and inducing lower CO_2 emissions than traditional ones, while providing the same reliability, with a much better durability. Considering the superior properties of UHPC, for which the cross section area of the structure can be slender and the total cement consumption maybe reduced. Moreover, to further minimize the negative influence of UHPC on the sustainable development, one of the most effective methods is to reduce the cement amount, without any significant scarification of the mechanical properties. From the available literature, it can be found that an optimal packing of granular ingredients is the key for a strong and durable concrete [18–20]. Hence, utilization of optimal packing models to design and produce the UHPC should be a possible way to reduce the cement amount and increase the cement efficiency.

Consequently, based on these premises, the objective of this study is to investigate the effect of nano-silica on the hydration and microstructure development of UHPC with low binder amount. The design of the concrete mixtures is based on the aim to achieve a densely packed material, by employing the modified Andreasen and Andersen particle packing model. The properties of the designed concrete, including the fresh and hardened behavior are evaluated in this study. Techniques such as isothermal calorimetry, thermal analysis and scanning electron microscopy are employed to evaluate the cement hydration and microstructure development of the UHPC.

2. Materials and experimental methodology

2.1. Materials

The cement used in this study is Ordinary Portland Cement (OPC) CEM I 52.5 R, provided by ENCI (the Netherlands). A polycarboxylic ether based superplasticizer is used to adjust the workability of UHPC. The limestone and quartz powder are used as fine fillers. Two types of sand are used, one is normal sand with the fractions of 0–2 mm and the other one is microsand with the fraction 0–1 mm (Graniet-Import Benelux, the Netherlands). A nano-silica slurry is selected as pozzolanic material to be used in this study. Short straight steel fibers (length of 13 mm and diameter of 0.2 mm) are employed to further improve the mechanical properties of the designed concrete. The detailed information about the used materials is summarized in Table 1 and Fig. 1. Additionally, the characterization and chemical analysis of the used nano-silica are shown in Tables 2 and 3, respectively.

2.2. Experimental methodology

2.2.1. Mix design of UHPC

For the design of mortars and concretes, several mix design tools are in use. Based on the properties of multimodal, discretely sized particles, De Larrard and Sedran [21,22] postulated different approaches to design concrete: the Linear Packing Density Model (LPDM), Solid Suspension Model (SSM) and Compressive Packing Model (CPM). Fennis et al. [23] have developed a concrete mix design method based on the concepts of De Larrard and Sedran [21,22]. However, all these design methods are based on the packing fraction of individual components (cement, sand, etc.) and their combinations, and therefore it is complicated to include very fine particles

Table 1
Properties of the used materials.

Materials	Specific density (g/cm^3)	Solid content (% w/w)	pH
CEM I 52.5 R	3.15	–	–
Limestone powder	2.71	–	–
Quartz powder	2.66	–	–
Microsand (sandstone)	2.72	–	–
Sand 0–2	2.64	–	–
Superplasticizer	1.05	35	7.0
Steel fiber	7.80	–	–

Table 2
Characterization of the used nano-silica.[a]

Type	Slurry
Stabilizing agent	Ammonia
Specific density (g/cm^3)	2.2
pH (at 20 °C)	9.0–10.0
Solid content (% w/w)	20
Viscosity (mPa s)	⩽100
BET (m^2/g)	22.7
PSD by LLS (μm)	0.05–0.3
Mean particle size (μm)	0.12

[a] Data obtained from the supplier.

in these mix design tools, as it is difficult to determine the packing fraction of such very fine materials or their combinations. Another possibility for mix design is offered by an integral particle size distribution approach of continuously graded mixes, in which the extremely fine particles can be integrated with a relatively lower effort, as detailed in the following.

Based on the investigation of Fuller and Thompson [24] and Andreasen and Andersen [25], a minimal porosity can be theoretically achieved by an optimal particle size distribution (PSD) of all the applied particle materials in the mix, as shown in the following equation:

$$P(D) = \left(\frac{D}{D_{max}}\right)^q \quad (1)$$

where $P(D)$ is a fraction of the total solids being smaller than size D, D the particle size (μm), D_{max} the maximum particle size (μm), and q is the distribution modulus.

However, in Eq. (1), the minimum particle size is not incorporated, while in reality there must be a finite lower size limit. Hence, Funk and Dinger [26] proposed a modified model based on the Andreasen and Andersen equation. In this study, all the concrete mixtures are designed based on this so-called modified Andreasen and Andersen model, which is shown as follows [26]:

$$P(D) = \frac{D^q - D_{min}^q}{D_{max}^q - D_{min}^q} \quad (2)$$

where D_{min} is the minimum particle size (μm).

The modified Andreasen and Andersen packing model has already been successfully employed in optimization algorithms for the design of normal density concrete [20] and lightweight concrete [27,28]. Different types of concrete can be designed using Eq. (2) by applying different value of the distribution modulus q, as it determines the proportion between the fine and coarse particles in the mixture. Higher values of the distribution modulus ($q > 0.5$) lead to coarse mixture, while lower values ($q < 0.25$) result in concrete mixes which are rich in fine particles [29]. Brouwers [30,18] demonstrated that theoretically a q value range of 0–0.28 would result in an optimal packing. Hunger [20] recommended using q in the range of 0.22–0.25 in the design of SCC. Hence, in this study, considering that a large amount of fine particles are utilized to produce UHPC, the value of q is fixed at 0.23, as shown in [51,52].

In this research, the modified Andreasen and Andersen model (Eq. (2)) acts as a target function for the optimization of the composition of mixture of granular materials. The proportions of each individual material in the mix are adjusted until an optimum fit between the composed mix and the target curve is reached, using an optimization algorithm based on the Least Squares Method (LSM), as presented in Eq. (3). When the deviation between the target curve and the composed mix, expressed by the sum of the squares of the residuals (RSS) at defined particle sizes, is minimized, the composition of the concrete is treated as the best one [19]:

Table 3
Chemical analysis of the used cement and nano-silica.

Substance	Cement (mass%)	Nano-silica slurry (mass%)
Al_2O_3	4.80	0.367
SiO_2	20.27	98.680
Na_2O	0.26	0.315
P_2O_5	–	0.220
K_2O	0.53	0.354
CaO	63.71	0.089
TiO_2	–	0.007
Fe_2O_3	3.43	0.004
CuO	–	0.001
ZrO_2	–	0.003
Ag_2O	–	0.022
MgO	1.58	–
SO_3	2.91	–
Cl^-	–	0.037
L.O.I.	2.51	–

$$RSS = \sum_{i=1}^{n}\left(P_{mix}\left(D_i^{i+1}\right) - P_{tar}\left(D_i^{i+1}\right)\right)^2 \quad (3)$$

where P_{mix} is the composed mix and P_{tar} is the target grading calculated from Eq. (2).

According to the optimized particle packing model, the developed UHPC mixtures are listed in Table 4. It can be noticed that the cement amount of the UHPC is relatively low, around 440 kg/m^3. Moreover, large amount of powder materials (limestone and quartz powder) are utilized to replace cement in this study. Based on the results presented in [53], the used powder materials are not considered as binder in the concrete. Furthermore, the nano-silica is added in the amount of 1%, 2%, 3%, 4% and 5% as a cement replacement. Hence, based on the results of the fresh

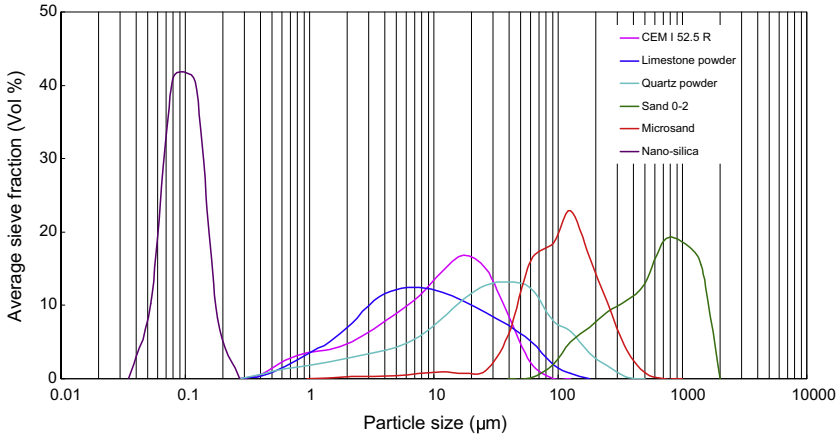

Fig. 1. Particle size distribution of the used materials.

Table 4
Mix recipe of the UHPC with nano-silica.

	Cement (kg/m^3)	Limestone (kg/m^3)	Quartz (kg/m^3)	Microsand (kg/m^3)	Sand 0–2 (kg/m^3)	Nano-silica (kg/m^3)	Water (kg/m^3)	SP (kg/m^3)
Ref.	439.5	263.7	175.9	218.7	1054.7	0	175.8	43.9
UHPC-1%	435.1	263.7	175.9	218.7	1054.7	4.4	175.8	43.9
UHPC-2%	430.7	263.7	175.9	218.7	1054.7	8.8	175.8	43.9
UHPC-3%	426.3	263.7	175.9	218.7	1054.7	13.2	175.8	43.9
UHPC-4%	421.9	263.7	175.9	218.7	1054.7	17.6	175.8	43.9
UHPC-5%	417.5	263.7	175.9	218.7	1054.7	22.0	175.8	43.9

and hardened properties of the designed UHPC, it is possible to evaluate the influence of nano-silica on the properties of UHPC. An example of the target curve and the resulting integral grading curve of the UHPC is shown in Fig. 2.

Additionally, Table 5 shows characteristics of each recipe listed in Table 4, which indicates the water/cement ratio, water/binder ratio, water/powder ratio, SP content by the weight of cement and SP content by the weight of powder. Due to the fact that a large amount of cement has already been replaced by limestone and quartz powder, the water to cement ratio is relatively high (about 0.4). However, the water/powder ratios of all the batches are still relatively low (around 0.18). Considering that the used water can be significantly absorbed by the powder materials, the SP amount by the weight of powder is fixed at about 4.5%. Finally, to further improve the mechanical properties of the UHPC, around 2.5% (vol.) steel fibers are added into the designed concrete matrix.

Table 5
Characteristics of the designed concrete recipes.

	w/c	w/b	w/p	SP content (% bwoc)	SP content (% bwop)
Ref.	0.400	0.400	0.180	9.987	4.486
UHPC-1%	0.404	0.400	0.180	10.090	4.486
UHPC-2%	0.408	0.400	0.180	10.193	4.486
UHPC-3%	0.412	0.400	0.180	10.298	4.486
UHPC-4%	0.417	0.400	0.180	10.405	4.486
UHPC-5%	0.421	0.400	0.180	10.515	4.486

w: water, c: cement, b: binder, p: powder (particle size < 125 μm), bwoc: by the weight of cement, bwop: by the weight of powder.

2.2.2. Mixing procedures

In this study, all powder ingredients (particle size < 125 μm) and sand fractions are slowly blended for 30 s in a dry state. Then, nano-silica slurry and around 75% of the total amount of water are slowly added and mixed for another 90 s. After that, the mixing is stopped for 30 s, in which the first 20 s are used to scratch the materials from the wall of the mixing bowl and the paddle. Afterwards, the remaining mixing water and superplasticizer are added into the mixer, during the consecutive mixing for 180 s at slow speed. For the samples with steel fibers, about 2.5% (vol.) of short steel fibers are added when a flowable UHPC matrix is obtained. The last step is mixing for 120 s at high speed. The mixing is always executed under laboratory conditions with dried and tempered aggregates and powder materials. The room temperature while mixing, testing and casting is constant at around 20 ± 1 °C.

2.2.3. Workability

After mixing, the suspension is filled into a conical mold in the form of a frustum (as described in EN 1015-3 [29]). During the test, the cone is lifted straight upwards in order to allow free flow for the paste without any jolting. In the test, two diameters perpendicular to each other are determined. Their mean is recorded as the slump flow value of the designed UHPC.

2.2.4. Air content

The air content of UHPC is experimentally determined following the subsequent procedure. The fresh mixes are filled in cylindrical container of known volume and vibrated for 30 s. The exact volume of the containers is determined beforehand using demineralized water of 20 °C. In order to avoid the generation of menisci at the water surface, the completely filled contained is covered with a glass plate, whose mass is determined before. Hence, based on the assumption that the fresh concrete is a homogeneous system, a possibility for determining the air content of concrete can be derived from the following equation:

$$\phi_{air} = \frac{V_{container} - V_{solid} - V_{liquid}}{V_{container}} \tag{4}$$

where ϕ_{air} is the air content (%, V/V) of UHPC, $V_{container}$ the volume of the cylindrical container that mentioned before, and V_{solid} and V_{liquid} are the volume of solid particles and liquid in the container (cm^3).

As the composition of each mixture is known, the mass percentage of each ingredient can be computed. Because it is easy to measure the total mass of concrete in the container, the individual masses of all materials in the container can be obtained. Applying the density of the respective ingredients, the volume percentages of each mix constituent can be computed. Hence,

$$V_{solid} = \sum_i \frac{M_i}{\rho_i} \tag{5}$$

and

$$V_{liquid} = \sum_j \frac{M_j}{\rho_j} \tag{6}$$

where M_i and ρ_i are the mass (g) and density (g/cm^3) of the fraction i in solid materials, M_j and ρ_j are the mass (g), and density (g/cm^3) of the fraction j in liquid materials, respectively. The schematic diagram for calculating the air content in concrete is shown in Fig. 3.

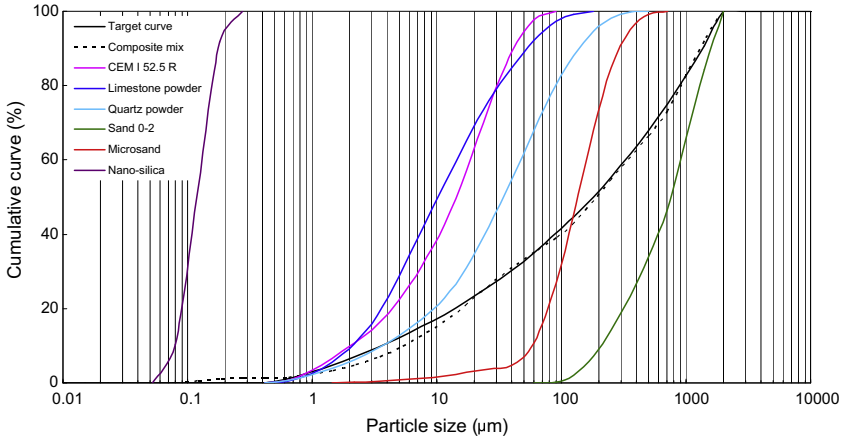

Fig. 2. PSDs of the ingredients, the target and optimized grading curves of the UHPC (based on Eq. (2) with $q = 0.23$).

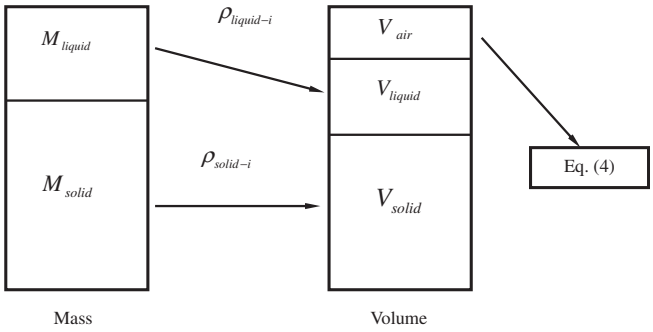

Fig. 3. Schematic diagram of the method to calculate the air content of UHPC in fresh state.

2.2.5. Mechanical properties

The concrete samples (with and without steel fibers) are cast in molds with the size of 40 mm × 40 mm × 160 mm. The prisms are demolded approximately 24 h after casting and then cured in water at about 20 ± 1 °C. After curing for 3, 7 and 28 days, the flexural and compressive strength of the specimens are tested according to the EN 196-1 [31]. At least three specimens are tested at each age to compute the average strength.

2.2.6. Porosity

The porosity of the hardened UHPC is measured applying the vacuum-saturation technique, which is referred to as the most efficient saturation method [32]. The saturation is carried out on at least 3 samples (100 mm × 100 mm × 20 mm) for each mix, following the description given in NT Build 492 [33] and ASTM C1202 [34]. The water permeable porosity is calculated from the following equation:

$$\varphi_{v,water} = \frac{m_s - m_d}{m_s - m_w} \cdot 100 \quad (7)$$

where $\varphi_{v,water}$ is the water permeable porosity (%), m_s the mass of the saturated sample in surface-dry condition measured in air (g), m_w hydrostatic mass of water-saturated sample (g), and m_d is the mass of oven dried sample (g).

2.2.7. Calorimetry analysis

Based on the recipes shown in Table 4, cement, limestone and quartz powder are mixed with silica slurry, superplasticizer and water. Nano-silica/binder mass ratios from 1% to 5% are investigated. Moreover, another reference sample (reference-2) with only cement and water (water/cement = 0.4) is simultaneously designed and prepared. All the pastes are mixed for 2 min and then injected into a sealed glass ampoule, which is then placed into the isothermal calorimeter (TAM Air, Thermometric). The instrument is set to a temperature of 20 °C. After 7 days, the measurement is stopped and the obtained data is analyzed. All results are ensured by double measurements (two-fold samples).

2.2.8. Thermal analysis

A Netzsch simultaneous analyzer, model STA 449 C, is used to obtain the thermo-gravimetric (TG) and differential scanning calorimetry (DSC) curves of concrete pastes. According to the recipes shown in Table 4, the pastes are produced without any aggregates. After curing in water for 28 days, the hardened samples are grinded to powder. Analyses are conducted at a heating rate of 10 °C/min from 20 °C to 1000 °C under flowing nitrogen.

Based on the TG test results, the hydration degree of the cement is calculated. Here, the loss-on-ignition (LOI) measurements of non-evaporable water content for hydrated UHPC paste are employed to estimate the hydration degree of cement [35]. Assuming that the UHPC paste is a homogeneous system, the non-evaporable water content is determined according to the following equation:

$$M'_{Water} = M_{105} - M_{1000} - M_{CaCO_3} \quad (8)$$

where M'_{Water} is the mass of non-evaporable water (g), M_{105} the mass of UHPC paste after heat treatment under 105 °C for 2 h (g), M_{1000} the mass of UHPC paste after heat treatment under 1000 °C for 2 h (g), and M_{CaCO_3} is the mass change of UHPC paste caused by the decomposition of $CaCO_3$ during heating (g). Then, the hydration degree of the cement in UHPC paste is calculated as:

$$\beta_t = \frac{M'_{Water}}{M_{Water\text{-}Full}} \quad (9)$$

where β_t is the cement hydration degree at hydration time t (%) and $M_{Water\text{-}Full}$ is the water required for the full hydration of cement (g). Based on the investigation results shown in [36], the value of $M_{Water\text{-}Full}$ employed in this study is 0.256.

2.2.9. Scanning electron microscopy analysis

Scanning electron microscopy (SEM) is employed to study the microstructure of UHPC. After curing for 28 days, the specimens are cut into small fragments and soaked in ethanol for over 7 days, in order to stop the hydration of cement. Subsequently, the samples are dried and stored in a sealed container before the SEM imaging.

3. Experimental results and discussion

3.1. Slump flow

The slump flow of fresh UHPC mixes versus the amount of nano-silica is depicted in Fig. 4. The data illustrates the direct relation between the nano-silica amount and the workability of fresh UHPC. It is important to notice that with the addition of nano-silica, the slump flow of fresh UHPC decreases linearly. For the UHPC developed here, the slump flow value of the reference sample is 33.75 cm, which sharply drops to about 22.5 cm when about 5% of nano-silica is added. This behavior is in accordance with the results shown in [10], which indicates that the addition of nano-silica greatly increases the water demand of cementitious mixes. One hypothesis explaining this is that the presence of nano-silica decreases the amount of lubricating water available within the interparticle voids, which causes an increase of the yield stress and plastic viscosity of concrete [10]. Hence, in this study, the plastic viscosity of UHPC significantly increases with an increase of the nano-silica amount, which in turn causes that its workability obviously decreases.

3.2. Air content and porosity

The air content of UHPC in fresh state and the porosity of UHPC in hardened state are presented in Fig. 5. As can be observed, the air content of the reference sample (without nano-silica) is relatively low (2.01%), which should be attributed to the dense particle packing of the designed UHPC. However, with an increasing amount of nano-silica, the air content of UHPC clearly increases. When the additional nano-silica amount is about 5%, the air content in fresh UHPC sharply increases to about 3.5%. To interpret this phenomenon, the effect of nano-silica on the viscosity of UHPC should be considered. With an increasing amount of nano-silica, the viscosity of UHPC significantly increases [10], which cause that the entrapped air cannot easily escape from the fresh concrete. Hence, the air content of the fresh concrete with high content of nano-silica is relatively larger.

Compared to the air content results, the porosity of hardened UHPC show very different development tendency. With an addition of nano-silica, the porosity of UHPC firstly decreases, and then slightly increases after reaching a critical value. In this study, the porosity of reference sample is about 10.5%, and sharply decreases

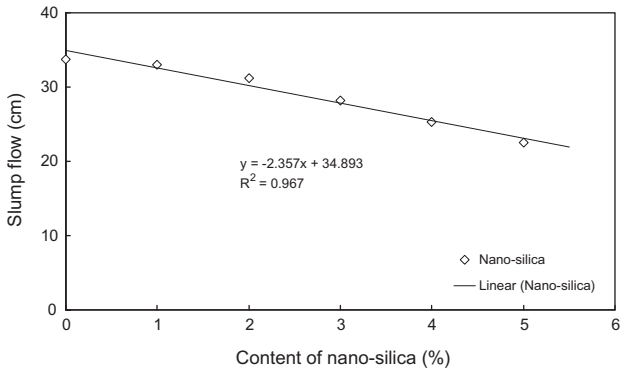

Fig. 4. Slump flow of UHPC at different nano-silica additions.

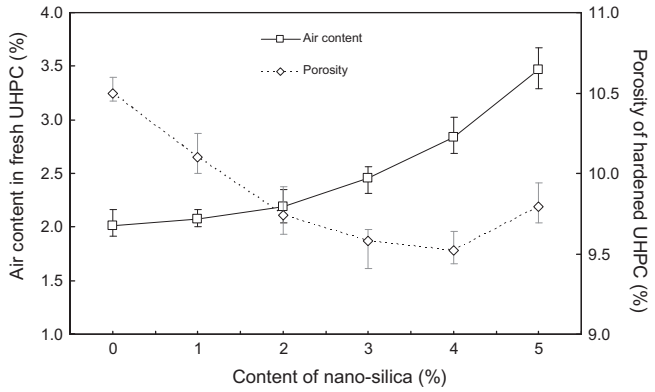

Fig. 5. Air content and porosity of UHPC with different amounts of nano-silica.

to about 9.5% when 4% of nano-silica is added. However, the porosity of the sample with 5% of nano-silica increases to about 9.8% again. This phenomenon should be attributed to the positive effect of nano-silica on the cement hydration. As commonly known, due to the nucleation effect of nano-silica, the formation of C–S–H-phase is no longer restricted on the grain surface alone, which cause that the hydration degree of cement is higher and more pores can be filled by the newly generated C–S–H [12]. For this reason, the porosity of UHPC firstly decreases with the addition of nano-silica. However, due to the fact that the air content of UHPC increases with the addition of nano-silica, the porosity of UHPC will increase again when the new generated C–S–H is insufficient to compensate the pores that are generated by the entrapped air in fresh concrete. Consequently, considering these two opposite processes, there is an optimal value of the nano-silica amount at which the lowest porosity of UHPC can be obtained.

3.3. Mechanical properties

The flexural and compressive strengths of UHPC at 3, 7 and 28 days versus the nano-silica amounts are shown in Fig. 6. With the addition of nano-silica, the parabolic growth tendency of the flexural and compressive strength of UHPC can be observed. For example, the flexural strength of reference sample at 28 days is about 10.4 MPa, which gradually increase to about 14.0 MPa when 4% of nano-silica is added. Afterward, this value slightly decreases to about 13.2 MPa when 5% of nano-silica is included. Hence, there should be an optimal amount of nano-silica, at which the flexural or compressive strengths of the designed UHPC can theoretical be the largest.

According to the regression equation of each parabola shown in Fig. 6, it is easy to understand that when the differential coefficient (y') of each function equals zero, the value of x represent the optimal nano-silica amount to obtain the best mechanical properties. Hence, the optimal nano-silica amount and the computed maximum flexural and compressive strengths at 3, 7 and 28 days are shown in Table 6. As can be seen, the optimal nano-silica amount for the flexural strength at 3, 7 and 28 days are 3.72%, 3.46% and 3.70%, respectively, which increase to 3.92%, 3.90% and 4.29% for the compressive strength. Based on these optimal nano-silica amounts, the computed maximum strengths are 9.99 MPa, 12.46 MPa and 13.79 MPa for flexural strength and 56.99 MPa, 69.63 MPa and 88.93 MPa for the compressive strength. Moreover, it is important to notice that computed maximum compressive strength at 28 days is 88.93 MPa, which is even smaller than the one with 4% of nano-silica (91.29 MPa). This should be attributed to the deviation of the regression equation. As can be noticed that the coefficient of determination (R^2) of the one representing the

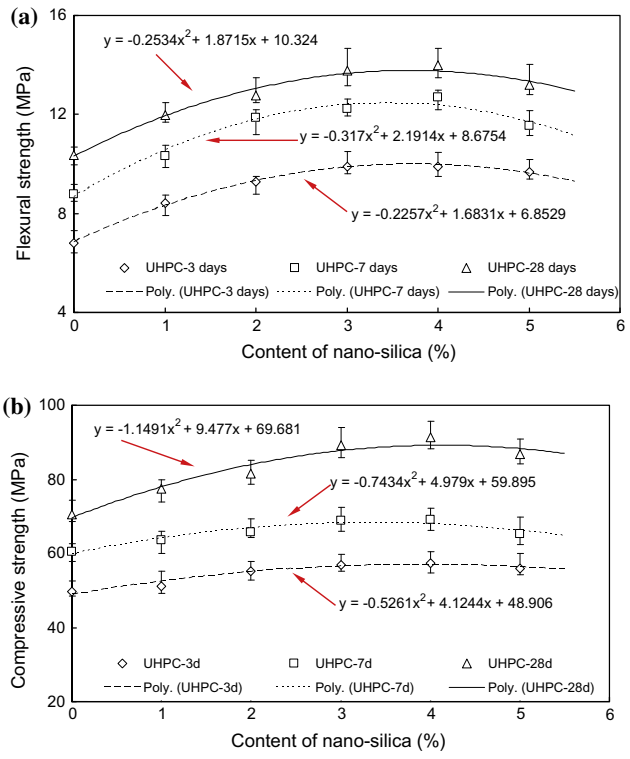

Fig. 6. Variation of the flexural (a) and compressive (b) strength of UHPC after curing for 3, 7 and 28 days as a function of nano-silica amount.

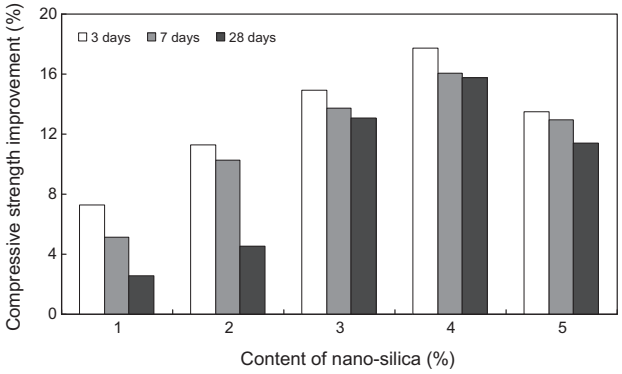

Fig. 7. Compressive strength improvement of UHPC with different nano-silica amount at 3, 7 and 28 days.

compressive strength at 28 days is only 0.862. Hence, to accurately obtain the optimal nano-silica amount in this study, only 3.72%, 3.46%, 3.70%, 3.92% and 3.90% are selected to calculate the average value (3.74%), which represents the optimal amount for this nano-silica in UHPC to theoretically get the best mechanical properties. This results are also in agreement with the results presented in Fig. 5.

In this study, to clearly show the advantages of the modified Andreasen and Andersen particle packing model in designing UHPC, the concept of the binder efficiency is utilized and shown as follows:

$$X_{binder} = \frac{f_c}{m_{binder}} \tag{10}$$

where X_{binder} is the binder efficiency, f_c the compressive strength of UHPC at 28 days, and m_{binder} is the total mass of the binders.

Table 6
Calculated optimal nano-silica amount for flexural and compressive strengths at 3, 7 and 28 days.

Calculated results	Flexural			Compressive		
	3 Days	7 Days	28 Days	3 Days	7 Days	28 Days
Optimal nano-silica amount (%)	3.72	3.46	3.70	3.92	3.90	4.29
Computed maximum strength (MPa)	9.99	12.46	13.79	56.99	69.63	88.93
Coefficient of determination (R^2)	0.996	0.980	0.982	0.948	0.969	0.862

Table 7
Comparison of the binder efficiency of the UHPCs.

Reference	Binders (kg/m^3)				Water (kg/m^3)	28 Days compressive strength (MPa)	Binder efficiency (N/mm^2)/(kg/m^3)
	Cement	GGBS	Fly ash	Silica (micro/nano)			
Oertel et al. [13]	825.0	0.0	0.0	175.0	175.0	140.0	0.14
Zhao et al. [49]	500.0	0.0	350.0	150.0	160.0	92.0	0.09
Wang et al. [48]	810.0	0.0	0.0	90.0	162.0	138.0	0.15
Wang et al. [48]	630.0	180.0	0.0	90.0	162.0	123.0	0.14
Wang et al. [48]	450.0	360.0	0.0	90.0	162.0	110.0	0.12
Deeb et al. [47]	500.0	0.0	0.0	72.0	166.0	80.0	0.14
Yazici [50]	850.0	0.0	0.0	260.0	170.0	115.0	0.10
Ref.	439.5	0.0	0.0	0.0	175.8	78.0	0.18
UHPC-1%	435.1	0.0	0.0	4.4	175.8	79.9	0.18
UHPC-2%	430.7	0.0	0.0	8.8	175.8	81.5	0.19
UHPC-3%	426.3	0.0	0.0	13.2	175.8	89.2	0.20
UHPC-4%	421.9	0.0	0.0	17.6	175.8	91.3	0.21
UHPC-5%	417.5	0.0	0.0	22.0	175.8	86.9	0.20

Ref., UHPC-1%, UHPC-2%, UHPC-3%, UHPC-4% and UHPC-5% are the mixtures designed in this study, in which 1–5% means the nano-silica amount by the total mass of binders.

A comparison of the binder efficiencies between the available literature and results obtained in this study is shown in Table 7. As can be seen, the binder efficiency of the mixtures designed in this study is significantly higher than that presented in the literature. Hence, it can be concluded that by the utilization of modified Andreasen and Andersen particle packing model, a dense and homogeneous skeleton of UHPC can be obtained with a relatively low binder amount (about 440 kg/m^3), and the binders can be well utilized.

Additionally, to evaluate the promotive effect of the employed nano-silica on the mechanical properties of UHPC, the following equation is utilized [36]:

$$K_t = \frac{S_i - S_0}{S_0} \quad (i = 1, 2, 3, 4 \text{ and } 5) \tag{11}$$

where K_t (%) is the compressive strength improvement, S_i (MPa) the strength of the UHPC with nano-silica (and i represents the addition of nano-silica), and S_0 (MPa) is the strength of the reference UHPC without nano-silica.

The compressive strengths improvement ratios of UHPC mixtures versus the nano-silica amount are illustrated in Fig. 7. It can be seen that, similarly to the flexural and compressive strengths results, the compressive strength improvement firstly increase with the increase of the nano-silica amount, and them decrease. Moreover, the effect of the nano-silica in improving the compressive strength of UHPC is more efficient at 3 days, comparing to that at 7 and 28 days. This phenomenon also implies that nano-silica can significantly promote the early hydration process of cement in UHPC.

To further improve the mechanical properties of the designed UHPC, about 2.5% (vol.) steel fibers are added into the concrete matrix. The flexural and compressive strength of the designed UHPC reinforced with steel fibers are shown in Fig. 8. It is clear to note that the addition of steel fiber can significantly improve the mechanical properties of the UHPC, whose flexural and compressive strength at 28 days can even reach around 25 and 135 MPa, respectively.

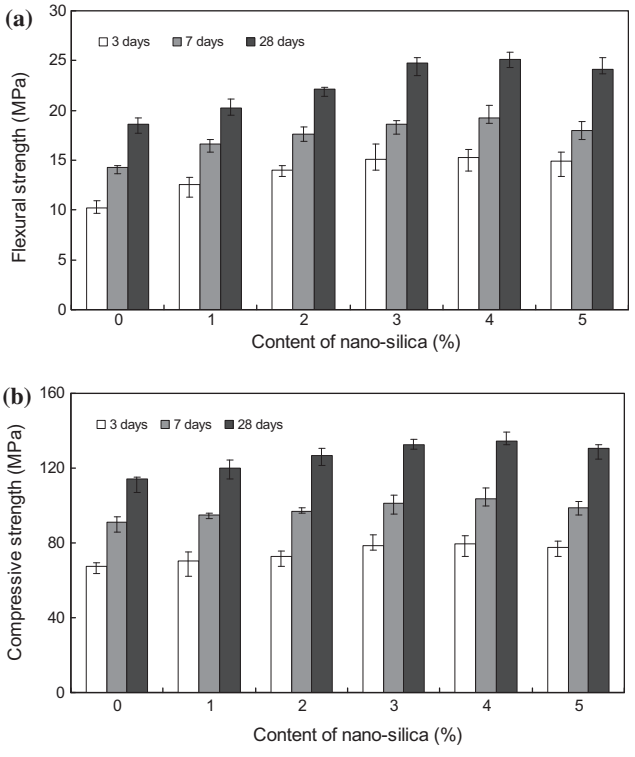

Fig. 8. Flexural (a) and compressive (b) strength of the designed UHPC with 2.5% (vol.) steel fibers.

3.4. Calorimetry test results

Based on the calorimetry test results, the influence of the nano-silica additions on the cement hydration of UHPC is analyzed. From Fig. 9, it is apparent that with an increase of the nano-silica

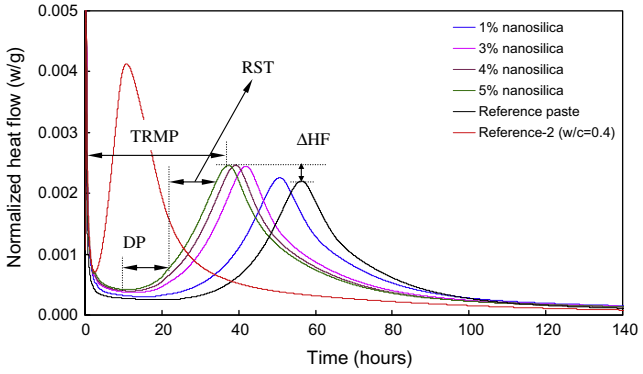

Fig. 9. Calorimetry test results of UHPC pastes with different amount of nano-silica *(Reference-2 is the sample with only cement and water, the water to cement ratio is 0.4, TRMP: time to reach the maximum peak; DP: dormant period; ΔHF: change in heat flow RST: relative setting time).*

amount, the height of the early rate peak is increased and the time required to reach the maximum rate is simultaneously reduced. This is in good agreement with the results presented in [1]. After hydration begins, hydrate products diffuse and envelop nanoparticles as kernels, which can promote the cement hydration and make the cement matrix more homogeneous and compact [37]. Additionally, the time of reaching the main rate peak varies significantly with a change of the reactivity of the silicas, with more reactive pozzolans giving an earlier peak. Therefore, in this study, with an increase of the nano-silica amount, more reactive kernels will be generated during the hydration, and the time to reach the main rate peak will correspondingly decrease.

Additionally, it can be clearly noted that the dormant period for cement hydration in reference sample is relatively long, which is around 30 h. In normal cement hydration process (only cement and water), the dormant period last only about 1–2 h, as shown in Fig. 9 (Reference-2). This phenomenon observed in this study should be attributed to the retardation influence of the superplasticizer. According to the investigation of Jansen et al. [38], complex Ca^{2+} ions from pore solution by the superplasticizer can touch the polymer absorbed on the nuclei or the anhydrous grain surfaces, which in turn might lead to the prevention of the growth of the nuclei or the dissolution of the anhydrous grains. Hence, due to a large amount of superplasticizer utilized to produce UHPC in this study, the cement hydration is significantly retarded, which also causes that the mechanical properties of reference UHPC are relatively poor at early age. Nevertheless, with the addition of nano-silica, the retardation effect from superplasticizer can be largely compensated. As shown in Fig. 9, with around 5% of nano-silica, the dormant period of cement hydration can be reduced to about 10 h.

3.5. Thermal test results

The TG/DSC curves for the UHPC with different amounts of nano-silica are presented in Fig. 10. From Fig. 10a, it is apparent that there main peaks exist in the vicinity of 105 °C, 450 °C and 800 °C for all the samples. As commonly known, the hydrated cement paste subjected to an elevated temperature loses the free water, dehydrates and the hydrated products are transferred [39–44]. Hence, the three peaks shown in Fig. 10a should be attributed to the evaporation of free water, decomposition of $Ca(OH)_2$ and decomposition of $CaCO_3$, respectively. Fig. 10b shows the mass losses of the UHPC samples due to temperature effects. It can be found that the mass loss of free water and ettringite in the reference sample is the lowest, and slightly increases with additions

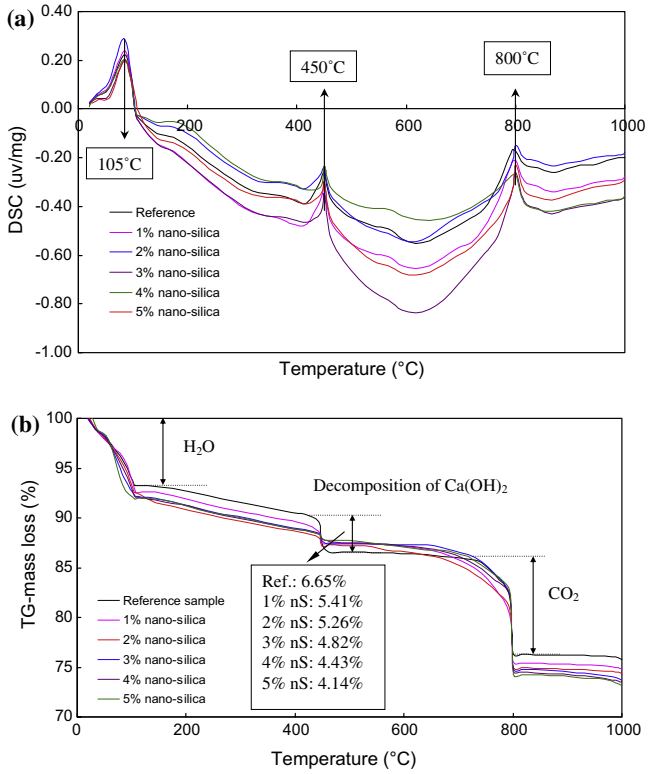

Fig. 10. TG/DSC curves for UHPC with different nano-silica amount: (a) DSC (deferential scanning calorimetry) and (b) TG (sample mass loss in percentage).

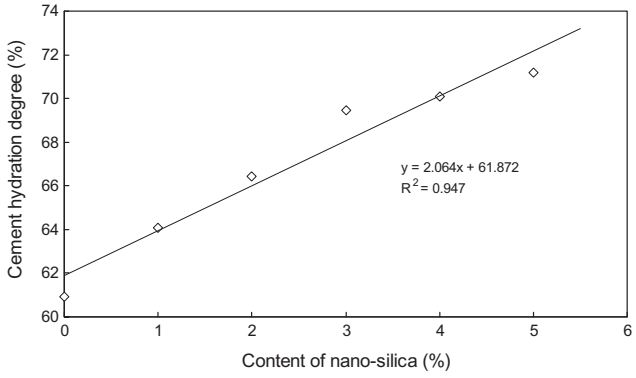

Fig. 11. Cement hydration degree of UHPC with different nano-silica amount (after curing for 28 days).

of nano-silica. Moreover, the mass loss of $Ca(OH)_2$ in the reference sample is the largest, which gradually reduces with an increasing nano-silica amount. These should be attributed to the following two points: (1) nano-silica can promote the hydration of cement and more hydration products (such as ettringite) can be produced and (2) nano-silica can react with $Ca(OH)_2$ to generate more C–S–H gel.

Additionally, based on the TG results and Eqs. (8) and (9), the hydration degree of the cement in UHPC paste after hydrating for 28 days is computed. As indicated in Fig. 11, with increasing amount of added nano-silica, the cement hydration degree linearly increases. As observed here, the cement hydration degree of the reference UHPC is about 57.1%, and increases to about 66.7% when a 5% addition of nano-silica is included. Moreover, it can be noticed that the hydration degree of the sample with 3%, 4% or 5% of

nano-silica are similar to each other, which means the promotion effect of nano-silica on cement hydration is not so strong anymore for nano-silica addition over 3% of the binder amount. This phenomenon is in agreement with the results shown in Fig. 9. Furthermore, it can also be found that the cement hydration degrees of all the designed UHPCs are larger than for other UHPCs found in the literature [45,46]. Normally, for the production of the UHPC, the water to binder ratio is low (less than 0.2), which causes that a large amount of cement particles is still unhydrated after 28 days. However, in this study, the binder amount in the UHPC is relatively low (about 440 kg/m^3), and significant amount of fillers are used to replace the cement, which cause that the water/cement ratio can be significantly increased with the same amount of water.

Combining the results of calorimetry test and thermal analysis, it can be concluded that, in the UHPC cementitious system, the addition of superplasticizer can obviously retard the dormant period of cement hydration. However, due to the fact that the nano-silica can significantly promote the hydration of cement, the retardation effect from superplasticizer can be largely compensated and the cement hydration degree at later age (around 28 days) is less affected.

3.6. Mechanism analysis of hydration and microstructure development

For normal cement grains, the initial hydration is largely limited to take place on the grain surface alone. With an ongoing hydration, the cement grain will be consumed and the hydration products that are deposited on the cement grain surface will grow thicker. With increasing curing time, due to the packed hydration products, the ionic transfer between the unhydrated cement particle and the surrounding solution is quite difficult, which limits cement hydration and generation of a dense C–S–H structure. In the present study, the hydration of the reference sample should be similar to such a process. Its porosity in hardened state is relatively high and the mechanical properties are comparatively low. When nano-silica is included into the hydration system of cement, an early pozzolanic reaction will take place on the silica surface to form C–S–H seeds [1,5] (as shown in Fig. 12a). Consequently, the formation of C–S–H-phase is no longer limited to occur on the grain surface alone, and more C–S–H gel can be generated. In this study, due to the complexation of Ca^{2+} ions from the pore solution and polymer from the superplasticizer, the dormant period of cement hydration in UHPC can be significantly retarded. However, the addition of nano-silica can efficiently compensate the retardation effect from superplasticizer.

Based on the obtained results, it can be found that the nano-silica amount is important for hydration and microstructure development of UHPC. As shown in Fig. 12b, when the amount of nano-silica is low (e.g. less than 2%), the amount of the new generated C–S–H seeds is low, which means that, to a large extent, most hydration still takes place on the surface of the cement particles. Hence, the porosity of the hardened cement matrix is still relatively large. When the amount of nano-silica is too high (e.g. 5% by the weight of binder), the sufficient amount of the generated C–S–H seeds can enable that the hydration products grow on their surfaces and result in a dense C–S–H gel. However, because the addition of nano-silica greatly increases the viscosity of cementitious mixes, a large amount of air can be entrapped into the cementitious system, which in turn increases the porosity of hardened concrete (as shown in Fig. 5). When the nano-silica amount is optimal, the positive effect of the nucleation and the negative influence of the entrapped air can be well balanced. Therefore, there is an optimal nano-silica amount, at which the porosity of UHPC can be the lowest.

3.7. SEM analysis of hardened UHPC

Scanning electron microscopy (SEM) is employed to study the morphology and microstructure of the reference sample and the samples with nano-silica additions. In Fig. 13a (reference sample), a large amount of well-developed $Ca(OH)_2$ plates can be observed, which implies that without nano-silica, the porosity of the hardened

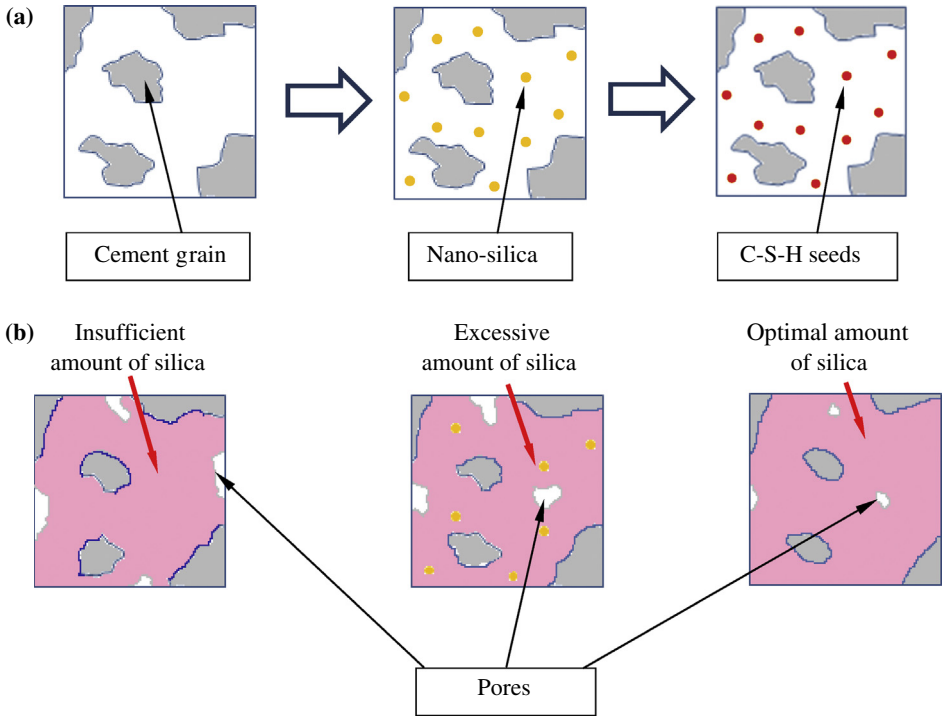

Fig. 12. Schematic diagram of the nucleation effect of nano-silica on UHPC: (a) mechanism of the generation of C–S–H seeds and (b) effect of the nano-silica amount on the microstructure development and porosity of UHPC.

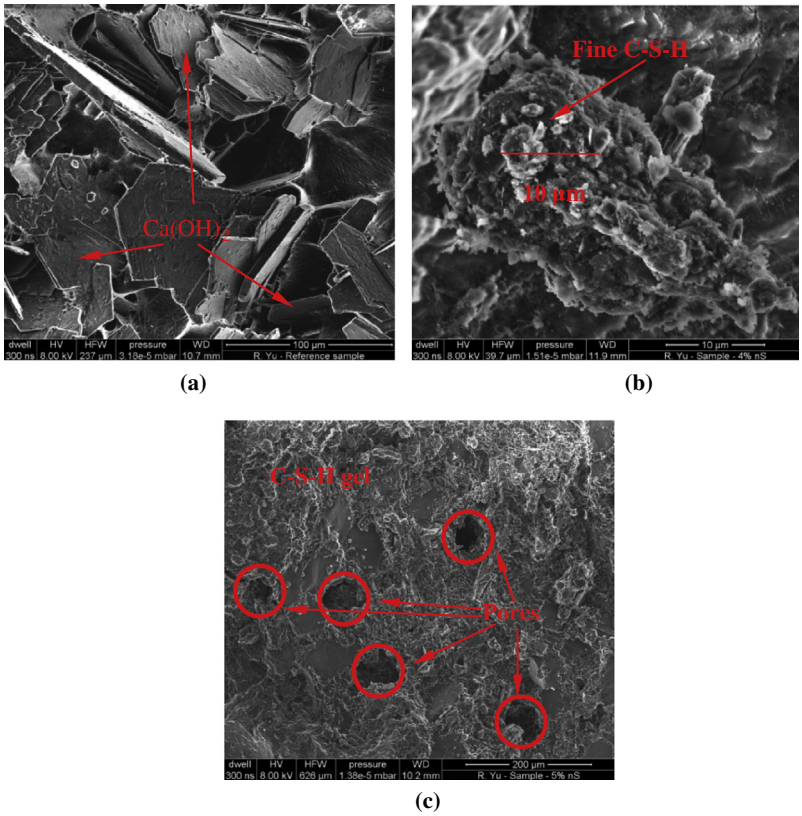

Fig. 13. SEM images: (a) reference sample, (b) UHPC with 4% of nano-silica, and (c) UHPC with 5% of nano-silica.

concrete is relatively large and the $Ca(OH)_2$ has enough space to grow. In Fig. 13b (UHPC with 4% of nano-silica), one can observe a very dense structure in the hardened matrix with only a few air pores. The main hydration product of the cement matrix is the foil-like C–S–H gel, and no $Ca(OH)_2$ crystal can be easily found. Furthermore, fine C–S–H gel can be found, which is probably generated from the pozzolanic reaction of nano-silica with $Ca(OH)_2$. The microstructure of the specimen with 5% addition of nano-silica is presented in Fig. 13c, in which a number of pores can be observed. As explained previously, because the addition of nano-silica greatly increases the viscosity of cementitious mixtures, a large amount of air can be entrapped in the cementitious system, which in turn increases the porosity of hardened concrete.

4. Conclusions

This paper presents the effect of nano-silica on the hydration and microstructure development of Ultra-High Performance Concrete (UHPC) with a low binder amount. From the results presented in this paper the following conclusions are drawn:

- Using the modified Andreasen and Andersen particle packing model, a dense and homogeneous skeleton of UHPC can be obtained with a relatively low binder amount (about 440 kg/m^3). When mixed with about 2.5% (vol.) of steel fibers, the flexural and compressive strength of the reinforced UHPC are around 25 and 135 MPa.
- An optimal amount of the utilized nano-silica (3.74% by the mass of the binder amount found here) corresponds to the highest mechanical properties of UHPC.
- In this study, due to a large amount of superplasticizer utilized to produce UHPC, the hydration of cement is obviously retarded. However, the addition of nano-silica can significantly compensate this retardation effect.
- With the addition of nano-silica, the viscosity of UHPC significantly increases, which causes that more air voids are entrapped in the fresh mixtures and the porosity of the hardened concrete correspondingly increase. However, in contrary, due to the nucleation effect of nano-silica, the hydration of cement can be promoted and more C–S–H gel can be generated. Hence, there is an optimal nano-silica amount for the production of UHPC with the lowest porosity, at which the positive effect of the nucleation and the negative influence of the entrapped air can be well balanced.

Acknowledgements

The authors wish to express their gratitude to M.Sc. George Quercia for his help and to the following sponsors of the Building Materials research group at TU Eindhoven: Graniet-Import Benelux, Kijlstra Betonmortel, Struyk Verwo, Attero, Enci, Provincie Overijssel, Rijkswaterstaat Zee en Delta – District Noord, Van Gansewinkel Minerals, BTE, V.d. Bosch Beton, Selor, Twee "R" Recycling, GMB, Schenk Concrete Consultancy, Geochem Research, Icopal, BN International, Eltomation, Knauf Gips, Hess ACC Systems, Kronos, Joma, CRH Europe Sustainable Concrete Centre, Cement&BetonCentrum and Heros (in chronological order of joining).

References

[1] Madani H, Bagheri A, Parhizkar T. The pozzolanic reactivity of monodispersed nanosilica hydrosols and their influence on the hydration characteristics of Portland cement. Cem Concr Res 2012;42(12):1563–70.
[2] Berra M, Carassiti F, Mangialardi T, Paolini AE, Sebastiani M. The pozzolanic reactivity of monodispersed nanosilica hydrosols and their influence on the hydration characteristics of Portland cement. Constr Build Mater 2012;35:666–75.

[3] Hou P, Kawashima S, Wang K, Corr DJ, Qian J, Shah SP. Effects of colloidal nanosilica on rheological and mechanical properties of fly ash–cement mortar. Cem Concr Compos 2013;35(1):12–22.
[4] Schmidt M, Amrhein K, Braun T, Glotzbach C, Kamaruddin S, Tänzer R. Nanotechnological improvement of structural materials – impact on material performance and structural design. Cem Concr Compos 2013;36:3–7.
[5] Land G, Stephan D. The influence of nano-silica on the hydration of ordinary Portland cement. J Mater Sci 2011;47(2):1011–7.
[6] Björnström J, Martinelli A, Matic A, Börjesson L, Panas I. Accelerating effects of colloidal nano-silica for beneficial calcium-silicate-hydrate formation in cement. Chem Phys Lett 2004;392(1–3):242–8.
[7] Shih JY, Chang TP, Hsiao TC. Effect of nanosilica on characterization of Portland cement composite. Mater Sci Eng A 2006;424(1–2):266–74.
[8] Nazari A, Riahi S. The effects of SiO_2 nanoparticles on physical and mechanical properties of high strength compacting concrete. Compos Eng 2011;42(3):570–8.
[9] Li H, Xiao H, Yuan J, Ou J. Microstructure of cement mortar with nano-particles. Compos Eng 2004;35(2):185–9.
[10] Senff L, Hotza D, Lucas S, Ferreira VM, Labrincha JA. Effect of nano-SiO_2 and nano-TiO_2 addition on the rheological behavior and the hardened properties of cement mortars. Mater Sci Eng A 2012;532:354–61.
[11] Ltifi M, Guefrech A, Mounanga P, Khelidj A. Experimental study of the effect of addition of nano-silica on the behaviour of cement mortars. Proc Eng 2011;10:900–5.
[12] Thomas JJ, Jennings HM, Chen JJ. Influence of nucleation seeding on the hydration mechanisms of tricalcium silicate and cement. J Phys Chem C 2009;113(11):4327–34.
[13] Oertel T, Hutter F, Tänzer R, Helbig U, Sextl G. Primary particle size and agglomerate size effects of amorphous silica in ultra-high performance concrete. Cem Concr Compos 2013;37:61–7.
[14] Kong D, Du X, Sun W, Zhang H, Yang Y, Shah SP. Influence of nano-silica agglomeration on microstructure and properties of the hardened cement-based materials. Constr Build Mater 2012;37:707–15.
[15] UNSTATS. Greenhouse gas emissions by sector (absolute values). United Nation Statistical Division. Springer; 2010.
[16] Friedlingstein P, Houghton RA, Marland G, Hackler J, Boden TA, Conway TJ, et al. Uptake on CO_2 emissions. Nat Geosci 2010;3:811–2.
[17] Habert G, Denarié E, Šajna A, Rossi P. Lowering the global warming impact of bridge rehabilitations by using ultra high performance fibre reinforced concretes. Cem Concr Compos 2013;38:1–11.
[18] Brouwers HJH, Radix HJ. Self compacting concrete: theoretical and experimental study. Cem Concr Res 2005;35:2116–36.
[19] Hüsken G. A multifunctional design approach for sustainable concrete with application to concrete mass products. PhD thesis. Eindhoven University of Technology, Eindhoven, The Netherlands; 2010.
[20] Hunger M. An integral design concept for ecological self-compacting concrete. PhD thesis. Eindhoven University of Technology, Eindhoven, The Netherlands; 2010.
[21] De Larrard F, Sedran T. Optimization of ultra-high-performance concrete by the use of a packing model. Cem Concr Res 1994;24:997–1009.
[22] De Larrard F, Sedran T. Mixture-proportioning of high-performance concrete. Cem Concr Res 2002;32:1699–704.
[23] Fennis SAAM, Walraven JC, den Uijl JA. The use of particle packing models to design ecological concrete. Heron 2009;54:185–204.
[24] Fuller WB, Thompson SE. The laws of proportioning concrete. Trans Am Soc Civil Eng 1907;33:222–98.
[25] Andreasen AHM, Andersen J. Über die Beziehungen zwischen Kornabstufungen und Zwischenraum in Produkten aus losen Körnern (mit einigen Experimenten). Kolloid-Z 1930;50:217–28 [in German].
[26] Funk JE, Dinger DR. Predictive process control of crowded particulate suspensions, applied to ceramic manufacturing. Boston, United States: Kluwer Academic Publishers; 1994.
[27] Yu QL, Spiesz P, Brouwers HJH. Development of cement-based lightweight composites – Part 1: mix design methodology and hardened properties. Cem Concr Compos 2013;44:17–29.
[28] Spiesz P, Yu QL, Brouwers HJH. Development of cement-based lightweight composites – Part 2: durability related properties. Cem Concr Compos 2013;44:30–40.
[29] Hüsken G, Brouwers HJH. A new mix design concept for each-moist concrete: a theoretical and experimental study. Cem Concr Res 2008;38:1249–59.
[30] Brouwers HJH. Particle-size distribution and packing fraction of geometric random packings. Phys Rev E 2006;74:031309-1–031309-14.
[31] BS-EN-196-1. Methods of testing cement – Part 1: determination of strength. British Standards Institution-BSI and CEN European Committee for Standardization; 2005.
[32] Safiuddin Md, Hearn N. Comparison of ASTM saturation techniques for measuring the permeable porosity of concrete. Cem Concr Res 2005;35:1008–13.
[33] NT Build 492. Concrete, mortar and cement-based repair materials: chloride migration coefficient from non-steady-state migration experiments. Nordtest Method, Finland; 1999.
[34] ASTM C1202. Standard test method for electrical indication of concrete's ability to resist chloride ion penetration. In: Annual book of ASTM standards, vol. 04.02. Philadelphia: American Society for Testing and Materials; July 2005.
[35] Bentz D, Feng X, Haecker C, Stutzman P. Analysis of CCRL proficiency cements 135 and 136 using CEMHYD3D. NIST internal report 6545; August 2000.
[36] Pane I, Hansen W. Investigation of blended cement hydration by isothermal calorimetry and thermal analysis. Cem Concr Res 2005;35:1155–64.
[37] Jalal M, Mansouri E, Sharifipour M, Pouladkhan AR. Mechanical, rheological, durability and microstructural properties of high performance self-compacting concrete containing SiO_2 micro and nanoparticles. Mater Des 2012;34:389–400.
[38] Jansen D, Neubauer J, Goetz-Neunhoeffer F, Haerzschel R, Hergeth WD. Change in reaction kinetics of a Portland cement caused by a superplasticizer – calculation of heat flow curves from XRD data. Cem Concr Res 2012;42(2):327–32.
[39] Alonso C, Fernandez L. Dehydration and rehydration processes of cement paste exposed to high temperature environments. J Mater Sci 2004;9(4):3015–24.
[40] Alarcon-Ruiz L, Platret G, Massieu E, Ehrlacher A. The use of thermal analysis in assessing the effect of temperature on a cement paste. Cem Concr Res 2005;35(3):609–13.
[41] Castellote M, Alonso C, Andrade C, Turrillas X, Campo J. Composition and microstructural changes of cement pastes upon heating, as studied by neutron diffraction. Cem Concr Res 2004;34(9):1633–44.
[42] Grattan-Bellew PE. Microstructural investigation of deteriorated Portland cement concretes. Constr Build Mater 1996;10(1):3–16.
[43] Handoo SK, Agarwal S, Agarwal SK. Physicochemical, mineralogical, and morphological characteristics of concrete exposed to elevated temperatures. Cem Concr Res 2002;32(7):1009–18.
[44] Bullard JW, Jennings HM, Livingston RA, Nonat A, Scherer GW, Schweitzer JS, et al. Mechanisms of cement hydration. Cem Concr Res 2011;41(12):1208–23.
[45] Van Tuan N, Ye G, Van Breugel K, Copuroglu O. Studies on hydration and microstructure of ultra high performance concrete incorporating rice husk ash. Cem Concr Res 2011;41(11):1–7.
[46] Van Tuan N, Ye G, Van Breugel K, Fraaij ALA, Bui DD. The study of using rice husk ash to produce ultra high performance concrete. Constr Build Mater 2011;25(4):2030–5.
[47] Deeb R, Ghanbari A, Karihaloo BL. Development of self-compacting high and ultra high performance concretes with and without steel fibres. Cem Concr Compos 2012;34:185–90.
[48] Wang C, Yang C, Liu F, Wan C, Pu X. Preparation of ultra-high performance concrete with common technology and materials. Cem Concr Compos 2012;34:538–44.
[49] Zhao S, Fan J, Sun W. Utilization of iron ore tailings as fine aggregate in ultra-high performance concrete. Constr Build Mater 2014;50:540–8.
[50] Yazici H. The effect of curing conditions on compressive strength of ultra high strength concrete with high volume mineral admixtures. Build Environ 2007;42:2083–9.
[51] Yu R, Spiesz P, Brouwers HJH. Mix design and properties assessment of Ultra-High Performance Fibre Reinforced Concrete (UHPFRC). Cem Concr Res 2014;56:29–39.
[52] Yu R, Tang P, Spiesz P, Brouwers HJH. A study of multiple effects of nano-silica and hybrid fibres on the properties of Ultra-High Performance Fibre Reinforced Concrete (UHPFRC) incorporating waste bottom ash (WBA). Constr Build Mater 2014;60:98–110.
[53] Kumar A, Oey T, Kim S, Thomas D, Badran S, Li J, et al. Simple methods to estimate the influence of LP fillers on reaction and property evolution in cementitious materials. Cem Concr Comp 2013;42:20–9.